NIST
National Institute of Standards and Technology
Technology Administration, U.S. Department of Commerce

NIST Technical Note 1533

Stable Optical Cavities for Wavelength References

Richard Fox
Kristan Corwin
Leo Hollberg

NIST Technical Note 1533

Stable Optical Cavities for Wavelength References

Richard Fox
Kristan Corwin
Leo Hollberg

Time and Frequency Division
Physics Laboratory
National Institute of Standards and Technology
325 Broadway
Boulder, CO 80305

May 2004

U.S. Department of Commerce
Donald L. Evans, Secretary

Technology Administration
Phillip J. Bond, Under Secretary for Technology

National Institute of Standards and Technology
Arden L. Bement, Jr., Director

Certain commercial entities, equipment, or materials may be identified in this document in order to describe an experimental procedure or concept adequately. Such identification is not intended to imply recommendation or endorsement by the National Institute of Standards and Technology, nor is it intended to imply that the entities, materials, or equipment are necessarily the best available for the purpose.

National Institute of Standards and Technology Technical Note 1533
Natl. Inst. Stand. Technol. Tech. Note 1533, 30 pages (May 2004)
CODEN: NTNOEF

Contents

Stable Optical Cavities for Wavelength References

Richard W. Fox, Kristan Corwin,* and Leo Hollberg

Time and Frequency Division
National Institute of Standards and Technology
Boulder, CO 80305

Abstract The use of stable, calibrated optical reference cavities to supply interferometer users with more precisely known optical wavelengths in air is considered. Several resonance wavelengths of an air-spaced ring cavity were determined by frequency measurements in a vacuum by use of a femtosecond-laser comb followed by corrections to account for atmospheric pressure and cavity temperature. A design of a new stable ring cavity is discussed that allows for the longitudinal mode index to be determined by difference-frequency measurements between the *S* and *P* polarized modes.

Keywords: femtosecond laser, frequency measurements, interferometry, wavelength standards.

*NIST Optoelectronics Division. Present address: Kansas State University, Dept. of Physics, Manhattan, KS 66506.

1. Introduction

Optical interferometers measure length in units of a known optical wavelength. Common interferometric systems use frequency-stable lasers, and the wavelength is a calculated parameter that depends on the local air's refractive index, which varies with air density and composition. Consequently, length measurements performed in air are substantially less accurate than similar measurements utilizing an interferometer operating in vacuum. A different approach that has been suggested is to frequency-lock a tunable laser to a mode of a mechanically stable reference cavity that is open to the air [1, 2, 3, 4]. Essentially, the frequency of a tunable laser is controlled to fix the wavelength in the medium. The wavelength may be determined by a calibration of some type, and known correction factors (such as the reference-cavity temperature) applied as necessary. Here, we have calibrated several modes of a prototype reference cavity by way of frequency measurements with a femtosecond-laser frequency comb. An additional feature of this reference-cavity approach is that several known wavelengths can be made available, enabling multiple–wavelength interferometry [5] to measure absolute distances with no moving retro-reflectors. Furthermore, by smoothly tuning between two known resonance wavelengths, swept-wavelength interferometry [6] is possible with no associated refractive index measurements.

A wavelength calibration of the cavity at a certain temperature can be accomplished indirectly by an optical frequency measurement. We can measure a tunable laser's frequency while it is locked to a resonance of the cavity in a vacuum chamber. The wavelength of the resonance in the vacuum may then be calculated with high precision since the limiting factor is not the refractive index but is instead likely to be the residual error of the temperature monitoring or offsets in the frequency-locking process. As discussed below, when air is re-introduced to the chamber the wavelength of each mode remains nominally the same, apart from several small corrections not related to the air's refractive index.

Subsequent frequency-locking of a laser to such a resonance will allow the user to know the laser wavelength in the reference cavity air path which, for instance, may be

placed adjacent to a length-measuring interferometer. Differences in the cavity temperature from the calibration temperature need to be properly accounted for, and therefore the cavity temperature must be monitored. However the cavity temperature measurements require much less precision than the air-temperature measurements to achieve the same wavelength accuracy. Monitoring the cavity temperature appears to be preferable to controlling it, since temperature control would unduly heat or cool the air in the cavity relative to the interferometer measurement path. Other correction factors include compensating for material contraction once the cavity is exposed to atmospheric pressure, and for any possible material aging. The correction for atmospheric pressure requires knowledge of the barometric pressure, but again not as precisely as the present method of using the Edlén equations [7]. The material aging issue refers to a gradual shrinking at the rate of $\Delta l/l \leq -5 \times 10^{-9}$ yr^{-1} in the low-expansion material ULE glass [8]. This characterization is the result of long-term measurements of Fabry-Perot resonance frequencies. Another candidate low-expansion glass material, Zerodur-M, exhibits an aging rate larger by an order of magnitude [9]. However the material contraction from vacuum to atmospheric pressure is half as large as that of ULE glass. Further discussion of these materials and a wavelength uncertainty error budget is presented later in this text.

Direct measurements of optical frequency as described here are to be distinguished from resonance frequency estimates based on measurements of the cavity free spectral range (FSR). Frequency measurements of a cavity's FSR to the level of 10^{-7} have been demonstrated at a single wavelength [10], but the FSR is wavelength dependent since the dielectric-mirror phase shift upon reflection is wavelength dependent. An accurate ($\Delta\nu/\nu \sim 10^{-8}$) measurement of a resonance frequency by way of FSR measurements does not appear to be practical at this point.

An implicit aspect of using a wavelength reference cavity that has been previously calibrated is that the particular mode with the previously measured wavelength must be somehow distinguished from adjoining modes. Transverse modes can be eliminated from consideration by proper alignment and spatial mode-matching to the cavity. However the tunable laser must be brought into coincidence and locked to the same longitudinal mode index m that was previously calibrated. Several methods of finding the correct mode are discussed in this report.

The choice of which laser to employ in this research has been based on several factors. Traditionally, most metrology systems have been built around the red 633 nm wavelength since frequency-stabilized He-Ne lasers have long been available. For this application we need a tunable laser with a line-width narrow enough to be captured and locked by electronic means. Tunable red extended-cavity diode lasers are an option; however, we have instead chosen to use telecom-band extended-cavity lasers and distributed-feedback (DFB) lasers during this initial work. While it is true that the longer wavelength is a negative factor with regard to an interferometric measurement, the DFB characteristics including ruggedness, power, cost, eye-safety, fiber compatibility and component availability are positive factors. Furthermore, for long measurement paths the longer wavelength is less important. For instance, for paths on the order of one meter, a very precise $\Delta l/l \sim 3 \times 10^{-8}$ measurement represents a fractional fringe interpolation of only 1/50 of a wave using the telecom-wavelength lasers.

To what extent can we expect to deliver a stable known wavelength by this method of calibrated reference cavities? The actual stability of the laser wavelength in air is a difficult parameter to measure. Monitoring the laser frequency via a heterodyne beat-note will only record changes of the air's refractive index. By building a rigid test interferometer and monitoring the apparent path length using our "stable wavelength," we are likely to measure a changing phase shift at some level. The question will then become, "Is the wavelength changing, or is the rigid test interferometer changing?" The solution may be to monitor a moderately stable low-expansion path length simultaneously by a vacuum interferometer (with a frequency-stabilized laser) in addition to the air-path measurement.

2. Wavelength Reference Cavity Considerations

2.1 Stability

Ring cavities are considered exclusively, as the problems associated with optical feedback from the cavity are greatly reduced. The resonance condition of an optical cavity is often approximated as an integer number of wavelengths in the cavity round-trip path length, or $m\lambda = L$. This simplification neglects any phase-shift upon reflection at the

mirrors. It also assumes plane-wave propagation, neglecting the phase accumulation that occurs as the optical wave diffracts. We write the resonance condition as

$$\lambda = \frac{L}{m + \frac{\varphi_m(\lambda) + \psi_R}{2\pi}} \quad , \tag{1}$$

where L is the physical round-trip path length of the ring resonator, the integer m is the longitudinal mode index, φ_m is the total phase-shift upon reflection from the dielectric mirrors per round-trip, and ψ_R is the total Gouy phase shift around the ring cavity [11].

Note that the index of refraction of the medium does not appear explicitly in Eq. (1). In other words, the resonant wavelength is to first order independent of the air density in the cavity. One may expect a higher-order dependence if the air affects $\varphi_m(\lambda)$, ψ_R, or L in any indirect manner. Examples would include a change of the cavity length L due to air pressure or mirror contamination. The largest sources of uncertainty appear to come from residuals after correcting for changes of the mechanical length L due to temperature, aging, and atmospheric pressure.

Equation (1) defines two distinct sets of modes, *s* and *p* polarized, that will in general have different resonance wavelengths since φ_m is polarization dependent due to the non-zero angle of incidence on the ring-cavity mirrors.

The total Gouy shift is the phase difference between a plane wave and the actual cavity mode wave, over a single round trip in the cavity. It is a function of the cavity geometry, i.e., the mirror curvatures and spacings. The shift may be calculated numerically for any cavity geometry, and will be a factor on the order of $\psi_R \sim 2\pi/5$ for all geometries considered here. For a two-mirror Fabry-Perot cavity, the Gouy term can be written as [12]

$$\psi_R = 2(1 + p + q)\cos^{-1}(\sqrt{g_1 g_2}) \quad , \quad g_i = 1 - \frac{L}{R_i} . \tag{2}$$

Here, p and q are the transverse mode indexes. As we will be interested only in the TEM_{00} modes, $p = q = 0$ for the designs considered in this report. The mechanical length L clearly enters Eq. (1) through the ψ_R term in the denominator, in addition to appearing explicitly in the numerator. However due to the large factor m (typically $>10^5$) in the

denominator of Eq. (1), this indirect contribution of cavity length drift to wavelength shift is quite small, far below the level of $\Delta\lambda/\lambda \sim 10^{-8}$. The ψ_R term can therefore be considered a constant for each cavity design considered here.

The phase shift upon reflection at each mirror is a function of mirror stack design. The coatings considered here are fabricated at elevated temperatures by ion-beam-assisted RF deposition, which results in nonporous layers that have virtually the same density as the bulk materials, Ta_2O_5 and SiO_2. Absorption of humidity is a known issue in the outer layers of porous coatings such as produced by e-beam sputtering, but ion-beam techniques are known to result in very stable multilayer coatings [13]. The coating layers will expand and contract with temperature in accordance with the bulk materials coefficient of expansion, but this is simply a small contribution to the overall cavity temperature response that will be measured at calibration as discussed later. Some gradual relaxation of the deposited amorphous material might be expected with time, but we expect this change to be on the order of a part per million or less. Since the effective coatings of even a four-mirror ring cavity represent a few parts in 10^5 of the entire path-length, we do not perceive coating instability as a problem that will contribute to $\Delta\lambda/\lambda$ at the 10^{-8} level in the $L \approx 25$ cm long cavities considered here.

In fact, we are considering cavities on the order of 25 cm in length in order to reduce the potential wavelength instability caused by mirror contamination. A molecular monolayer on each mirror of a ring cavity represents about 1 part in 10^8 of the path length. However, this does not equate to the wavelength instability caused by accumulating a monolayer of contamination. That depends on the additional phaseshift caused by the contamination, and would be on the order of $\Delta n l$, where Δn is the increase in the refractive index above the vacuum value and l is the layer thickness. We point out that the index of refraction is a bulk concept, and it would not be correct to assign $\Delta n = 0.3$ to a layer of water molecules for instance. It is very likely that the mirror surface, once exposed to room air, is covered with a layer of OH radicals, possible organics, and a subsequent monolayer of water molecules. An additional layer of water molecules is possible depending on the humidity [14]. At this point it is worth noting that the initial calibration does not need to be performed in a high-vacuum environment. Indeed, measuring the mode frequency with a background pressure of 0.1 Pa (~1 mTorr) will

cause an error (if uncorrected) of only $\Delta\lambda/\lambda \sim 2.3 \times 10^{-10}$. Consequently, since water is still very prevalent in vacuum chambers pumped down to only the 0.1 Pa range, we suspect that the calibration wavelength will include the effects of the hydroxyl and water mono-layers. We include a contribution of $\Delta\lambda/\lambda \leq \pm 1.0 \times 10^{-8}$ for mirror contamination in the error budget given in the following section. We also expect to have more quantifiable results after a series of experiments with several cavities operating in air.

To summarize the contributions of the dielectric mirror phase shift $\varphi_m(\lambda)$ and Gouy term ψ_R to the overall wavelength instability, these terms are significantly less than $\Delta\lambda/\lambda \sim 10^{-8}$. Wavelength uncertainty related to temperature, atmospheric pressure, and material aging are discussed in the following section concerning accuracy.

2.2 Accuracy

We are considering stable cavities made entirely of low-expansion glass with optically contacted mirrors. The goal is to construct a resonator with a wavelength uncertainty between calibrations of a few parts in 10^8 or better. The wavelength uncertainty provided to the interferometer user may then largely be a function of how well the refractive index of the air in the cavity matched that of the interferometer path. In this section we discuss the major contributions to the resonator's wavelength uncertainty.

As discussed in the introduction, candidates for mirror spacer material include ULE glass and Zerodur-M. The initial temperature coefficient at room temperature will be within the range of $\pm 30 \times 10^{-9}$ °C^{-1}. The temperature coefficient of each cavity would be measured during the femtosecond comb calibration over a nominal range of temperatures near room temperature. Subsequent use would entail monitoring the cavity temperature and correcting the wavelength as the cavity temperature deviates from the calibration temperature. We note that the temperature calibration will include the effects, if any, of a possible temperature coefficient of the dielectric mirrors.

The cavity's coefficient of expansion, $\alpha(T)$, will be approximated by fitting a polynomial to experimental data points derived from frequency measurements over a range of ±5 °C from room temperature. We expect to measure the coefficient of expansion $\alpha(T)$ at multiple temperatures over this limited range with an accuracy of $\pm 2 \times$

10^{-9} °C^{-1}. In the present experiment that uses 1500 nm wavelength lasers and mode widths of 4MHz, this level of uncertainty will require determining the resonant mode line-center to 400 kHz. The corrected wavelength would be estimated according to

$$\lambda(t) = \lambda_C (1 + \int_{T_C}^{T(t)} [\alpha(T) + \varepsilon] dT), \qquad (3)$$

where λ_C and T_C are the calibration wavelength and temperature, respectively, ε is the error of the polynomial approximation with respect to the true coefficient of expansion, and $T(t)$ is the temperature at time t. The error in the estimation of $\lambda(t)$ will have two independent components which will be combined in a root-sum-square (RSS) fashion to determine the total error caused by temperature. The first component is due to uncertainties in the temperature measurement during use, $T(t)$. Absolute temperature is not important, only the temperature change with respect to the calibration temperature T_c. Inexpensive semiconductor temperature sensors with long term stability better than ±0.1 °C are available, and we have chosen to permanently mount two of these to each wavelength reference cavity. Referring to the maximum error in the temperature measurement with respect to the calibration temperature as $\Delta T(t)$, we estimate the error in $\lambda(t)$ due to this component to be $\Delta T(t) \times \alpha(T)_{max}$, or $\Delta\lambda/\lambda \leq \pm 3 \times 10^{-9}$.

The second component is due to the error in approximating $\alpha(T)$, which is modeled in Eq. (3) as a constant error (ε) that is independent of temperature. The second component will scale with the temperature difference from calibration, increasing the uncertainty of the wavelength reference as the operating temperature range increases. We estimate the error in $\lambda(t)$ as $\varepsilon \times [T(t) - T_c]_{max}$, and define a narrow but useful operating temperature range of ±5 °C about the calibration temperature. For this component of the error we then have $\Delta\lambda/\lambda \leq \pm 1 \times 10^{-8}$ (assuming $\varepsilon \leq \pm 2 \times 10^{-9}$ °C^{-1} and $[T(t) - T_c]_{max} \leq 5$ °C). In summary we find that the temperature correction error is dominated by possible errors at the operating temperature extremes due to the error in approximating $\alpha(T)$. The total RSS error is estimated to be $\Delta\lambda/\lambda \leq 1.05 \times 10^{-8}$. In the error budget at the end of this section a conservative total uncertainty of $\Delta\lambda/\lambda \leq 2 \times 10^{-8}$ is allotted for errors in the correction for the temperature drift. We note that temperature hysteresis, which has been

observed in Zerodur [15], may be included in this discussion by increasing ε appropriately.

Long-term material contraction, or creep, is a known characteristic of ULE, Zerodur and Zerodur-M. This effect is larger in Zerodur, which is part crystalline and part amorphous glass. The contraction rate is known to be a function of time, decreasing as the material gets older. Previous experimental results are shown in Table 1. However the drift rate of Zerodur is also known to change with temperature variations of only a few degrees, meaning that even room temperature variations will place limitations on the longer-term wavelength predictability [15]. We focus here on ULE glass, which has an aging drift less by an order of magnitude than Zerodur. At this juncture there appears to be a trade-off between accuracy versus the time between calibrations. How accurate an air wavelength could be supplied between a typical calibration schedule of three years, for instance, when subject to typical room-temperature fluctuations? Data from a number of cavities subject to typical conditions will be required to answer that question. We have included in the $\Delta\lambda/\lambda$ uncertainty budget for a ULE cavity the conservative estimation of $\Delta\lambda/\lambda \leq \pm 0.5 \times 10^{-8}$ to account for the residual after the correction for the time since calibration.

As the wavelength calibration will be performed in vacuum, any change in the resonant wavelength with air pressure must be properly accounted for. There are two known effects that scale with pressure; the first is a bulk volume decrease due to the finite

Table 1. Aging rates of several low-expansion glasses from the references shown. All the results were collected over periods of at least 2 years except where noted. In some cases we have converted the reference data to yr^{-1} to facilitate comparison. The negative sign indicates the length change is in all cases a contraction.

Reference	ULE	Zerodur-M	Zerodur
Bergquist [16]	$\leq -2.4 \times 10^{-9}\ yr^{-1}$		
Marmet (1997) [17]	$\leq -3.7 \times 10^{-9}\ yr^{-1}$		
Hils (1989) [15]			$\leq -2 \times 10^{-7}\ yr^{-1}$
Tamm (2000) [18]	$\leq -5.5 \times 10^{-9}\ yr^{-1}$		
Riehle (1998) [19]		$\leq -3.2 \times 10^{-8}\ yr^{-1}$	$\leq -6.3 \times 10^{-8}\ yr^{-1}$

bulk modulus of the glass, and the second is a slight correction due to the dielectric mirror phase shift. According to theory the change in bulk volume causes a proportional change in length [20] that follows

$$\frac{\Delta l}{l} = \frac{1}{3}\frac{\Delta V}{V}. \tag{4}$$

The volume change is related to the pressure change by the bulk modulus K:

$$\frac{\Delta V}{V} = \frac{\Delta P}{K} = \frac{\Delta P}{E/[3(1-2\nu)]}. \tag{5}$$

In Eq. 5 the bulk modulus is written in terms of the modulus of elasticity (E) and Poisson's ratio (ν). Unfortunately for both Zerodur and ULE glass these quantities may vary slightly (by at least ±2 %, 1σ) from batch to batch. For Zerodur (nominal E = 90.3 GPa and ν = 0.243), the theory indicates a linear contraction of $\Delta l/l = 0.577 \times 10^{-6}$ from vacuum to one Atmosphere. For ULE (nominal E = 67.6 GPa and ν = 0.17), the theory indicates a linear contraction of $\Delta l/l = 0.989 \times 10^{-6}$.

There are at least three distinct approaches to correcting the reference wavelength to account for the material contraction. In brief these are:

- Calculate using the nominal material parameters. This method relies on the simple theory being applicable, and on the accuracy of the material parameters E and ν.
- Backfill the vacuum chamber with helium instead of air. The helium index of refraction may be calculated from theory more precisely than that of air, and used to calibrate the cavity contraction [21].
- Measure a known Fabry-perot interferometer path length using the wavelength reference. To be useful, the path length needs to be known within an uncertainty of a few parts in 10^8 or better.

We will use the second approach to estimate an uncertainty in the correction of the cavity contraction. In practice one could employ helium back-filling or simply measure the cavity mode frequency in a known pressure of helium. The refractive index of helium as a function of frequency and temperature is presently known theoretically with an uncertainty of approximately $\pm 3 \times 10^{-9}$ [21]. At near infrared wavelengths the value is approximately an order of magnitude smaller than that of air ($1-n \approx 2.5 \times 10^{-5}$ at 10^5 Pa). The temperature coefficient

is also smaller than that of air (helium: -1.1×10^{-7} °C^{-1} versus air: -9.4×10^{-7} °C^{-1}, at 1 atmosphere). The uncertainty of the cavity contraction calibration would be limited more or less equally by uncertainty contributions from the helium pressure and temperature measurements.

We estimate that the wavelength could be measured in 1 atmosphere of helium with an uncertainty of $\Delta\lambda/\lambda \leq \pm 2.7 \times 10^{-8}$, assuming that the gas temperature is known to ±0.2 °C and the pressure known to ±50 Pa. The temperature measurement would utilize high-resistance thermistors mounted on metal fins placed near the cavity optical path. The pressure measurement would be accomplished with a capacitance manometer (±0.05 % accuracy).

In subsequent use of the wavelength reference the absolute barometric pressure could be monitored with inexpensive sensors with an uncertainty of ±1.5 %. By itself the barometric error results in an uncertainty of approximately $\Delta\lambda/\lambda \leq 0.87 \times 10^{-8}$ (for Zerodur), and $\Delta\lambda/\lambda \leq 1.5 \times 10^{-8}$ (for ULE). Thus we combine the uncertainty of the wavelength shift with pressure with the uncertainty of barometric pressure and find the total pressure-related uncertainty terms of $\Delta\lambda/\lambda \leq 2.84 \times 10^{-8}$ (for Zerodur) and $\Delta\lambda/\lambda \leq 3.09 \times 10^{-8}$ (for ULE glass).

The second correction to be applied when the cavity experiences atmospheric pressure after being calibrated in vacuum relates to the dielectric mirror phase shift. $\varphi_m(\lambda)$ will change slightly with air pressure since the reflectivity of a dielectric mirror

Table 2. Uncertainty budget for a wavelength reference constructed from ULE.

Item	$\Delta\lambda/\lambda$
Temperature correction error	$\pm 2.0 \times 10^{-8}$
Aging correction error	$\pm 0.5 \times 10^{-8}$
Bulk volume change correction error	$\pm 3.1 \times 10^{-8}$
Mirror phase shift correction error	$\pm 0.001 \times 10^{-8}$
Mirror contamination uncertainty	$\pm 1.0 \times 10^{-8}$
Wavelength calibration uncertainty	$\pm 0.25 \times 10^{-8}$
Root-Sum-Square Total	$\pm 3.9 \times 10^{-8}$

depends on the surrounding index. Under normal barometric fluctuations this causes a negligible change of the wavelength stability ($\Delta\lambda/\lambda$), but is a factor on the order of 10^{-10} per mirror when the change is from vacuum to atmospheric pressure. For a four-mirror cavity, as discussed later in this report, the mirror phase-shift correction will be approximately a $\Delta\lambda/\lambda \sim 10^{-9}$ correction. The error of this correction will be governed by the accuracy of the pressure measurement (typically ±1 %), so we allot $\Delta\lambda/\lambda \leq 10^{-11}$ in the uncertainty budget for this effect.

In the uncertainty budget we also include a small term arising from the measurement of the cavity resonance wavelength. The actual measurement process, the result of frequency counting a beat-note made with the femtosecond comb, has an error much less than is relevant here. If the frequency locking process of the test laser to the stable cavity is able to control most of the laser's frequency fluctuations, so that a narrow line-width is produced, the pertinent error is the offset from the cavity line-center. If the bandwidth of the locking feedback loop is not large with respect to the initial laser line-width, then the heterodyne beat-note observed during calibration may be on the order of 2 MHz. In this case, the pertinent error may be how close the beat-note line-center can be estimated. Visually reading the beat-note frequency from a spectrum analyzer would represent the worst case, and we estimate an error of less than 500 kHz and write the contribution to the uncertainty budget as $\Delta\lambda/\lambda \leq \pm 0.25 \times 10^{-8}$.

2.3 Mode Discrimination

A small cavity is appealing since the free spectral range (FSR) would be large, which would facilitate the unambiguous identification of each mode. For instance, the *s* polarized TEM_{00} modes of a ring cavity with an 8 mm perimeter would be separated by 37.5 GHz. At red wavelengths, a laser frequency repeatability of about 50 ppm would be more than sufficient to return unambiguously to a given mode. However, such a small cavity is more vulnerable to environmental effects such as contamination of the mirror surface.

Due to these uncertainties we have considered longer cavities, on the order of 25 cm, in order to reduce the potential wavelength instability caused by possible contamination of the mirrors. However, longer cavities present a challenge in the unambiguous identification of a particular (previously calibrated) mode. There are a number of distinct approaches to accomplish the mode discrimination in a cavity of this size (L = 25 cm round-trip, 1.2 GHz free spectral range). The first is to rely on laser repeatability for a tunable laser to return to the same (previously calibrated) mode. This may be possible with certain types of lasers, for instance solid-state lasers. Secondly, another air-spaced optical reference cavity may be used, with a shorter length and lower resolution, and the coincidences between the two cavities will indicate the correct modes. This vernier approach is introduced in Fig. 1, below. The shorter cavity must be air-spaced since the frequency of the finely-spaced reference cavity modes may shift by more than a FSR with the ambient barometric pressure. The shorter cavity may be built in the same structure as the reference cavity [4]. It appears also possible to have the second cavity be physically separated from the high-finesse cavity, perhaps mounted in the laser box and connected by optical fiber. The use of a second-cavity approach to mode discrimination is appealing due to simplicity, although the extra optical cavity requires additional expense to construct and align.

An alternative approach to identifying the modes of the wavelength-stable cavity may be to utilize the frequency difference of the orthogonally polarized modes. The phase shift upon reflection of a non-normally incident beam is wavelength dependent, so with sufficient *s-to-p* dispersion each *s* and *p* longitudinal mode pair will have a unique and measurable frequency difference. The frequency difference may be enhanced by increasing the number of cavity mirrors with large angles of incidence. The most direct approach to measuring the frequency difference would be to use two lasers, one locked to each mode. In general, the precision of the *s-to-p* frequency difference measurement will be limited by the *p* mode line-width, $\Delta\nu_P$, since the reflectivity is not as high as that of the *s* polarization.

There are a number of designs for high-reflectivity dielectric coatings that exhibit different behavior of the phase-shift upon reflection. For this application the best coating

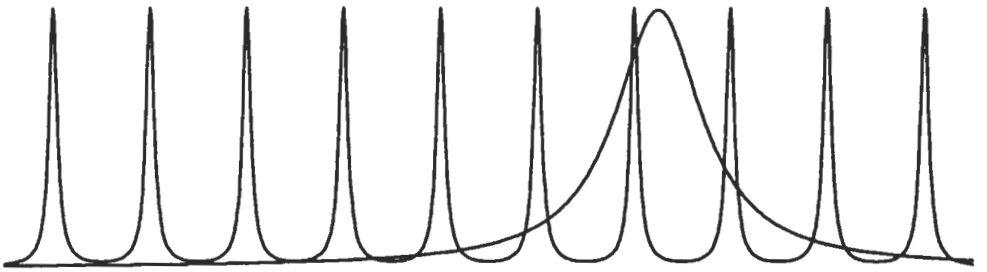

Figure 1. Mode identification using the two-cavity vernier technique. A short cavity with a large unambiguous free spectral range is used to identify a particular mode of a wavelength reference cavity. The short cavity must also be air-spaced.

design will optimize the *s-to-p* frequency difference per FSR in relation to the *p* polarized mode line-width $\Delta\nu_P$. This suggests a figure of merit, which we define below as Γ. We let $\Delta\nu_{sp}$ represent the difference in the longitudinal mode frequencies of the two polarizations, and $\Delta(\Delta\nu_{sp})$ is then the change in this mode spacing per free spectral range. Then we write

$$\Gamma = \frac{1}{3}\frac{\Delta\left(\Delta\nu_{sp}\right)}{\Delta\nu_{p}} \times 100\% . \tag{6}$$

This represents the precision that the frequency difference must be measured in relation to the limiting linewidth. For example, at a certain wavelength a cavity may have a *p* mode line-width of 2 MHz and an *s-to-p* frequency difference ($\Delta\nu_{sp}$) of approximately 100 MHz. Furthermore, $\Delta\nu_{sp}$ changes by 30 kHz every free spectral range due to the coating phase shifts. To unambiguously identify a particular mode of the cavity, we need to measure the frequency difference $\Delta\nu_{sp}$ to perhaps 1/3 of this interval, approximately 10 kHz. The pertinent quantity is therefore what percentage of the linewidth the 10 kHz represents. In this example, the line-center would have to be measured to 10 kHz out of 2 MHz, or a 0.5 % measurement.

2.4 Cavity Designs

It is useful then to explore different designs for the cavity and coating with the figure of merit Γ in mind. Other aspects to consider include spatial-mode shape, fabrication difficulty, and the number of (expensive) optical coating runs required.

2.4.1 Three-mirror cavity

We start with a three-mirror cavity that has the advantage of being astigmatically compensated (see Fig. 2). We analyze this using the same coating on all three mirrors, to avoid more than one expensive mirror-deposition run. There are many different coating designs, and we use here $H(LH)^n$ because the *s* and *p* polarizations have the same phase shift approximately mid-band (H and L refer respectively to the layers of high and low refractive index). This allows the difference frequency $\Delta\nu_{SP}$ between the two polarization modes to be on the order of a megahertz near the coating band center, which facilitates the measurement of kilohertz differences between cavity FSRs. (For instance, it may allow an inexpensive frequency-to-voltage converter to be used, with no intermediate IF stage). It also allows the cavity to be used as a reference for two relatively close (less than 100 MHz) optical frequencies, allowing the interferometer system designer very long synthetic wavelengths ($c/\Delta\nu > 3$ m).

We calculate the loss per pass by multiplying the reflectivity at each mirror. The round-trip reflectivity, along with the round-trip phase shift of each polarization is shown in Fig. 3 for an $H(LH)^{11}$ coating. (The exponent refers to the number of LH coating pairs). From the Fig. 3 data we calculate the *s* and *p* mode line-widths that a three-mirror cavity would have with a $H(LH)^{11}$ coating, assuming the ring cavity was 25 cm long and the loss was due primarily to the mirrors. These calculations are shown in Fig. 4. The figure of merit Γ is also plotted, and is on the order of 0.2 % near the center of the mirror pass-band. To discriminate modes using this frequency-difference technique would require measuring the center of the cavity mode to approximately ±0.2 %. In addition to the $H(LH)^n$ coating design, it is possible that other designs may offer more *s*-to-*p* polarization dispersion, which would increase the figure of merit Γ by a similar amount.

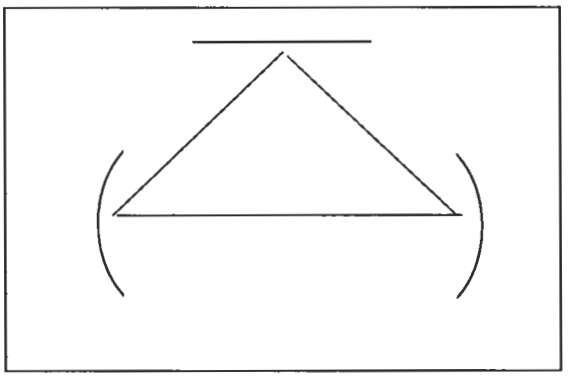

Figure 2. This three-mirror cavity has two reflections at a 22.5° angle of incidence and one at a 45° angle of incidence. The beam waist between the curved mirrors is round and free of astigmatism.

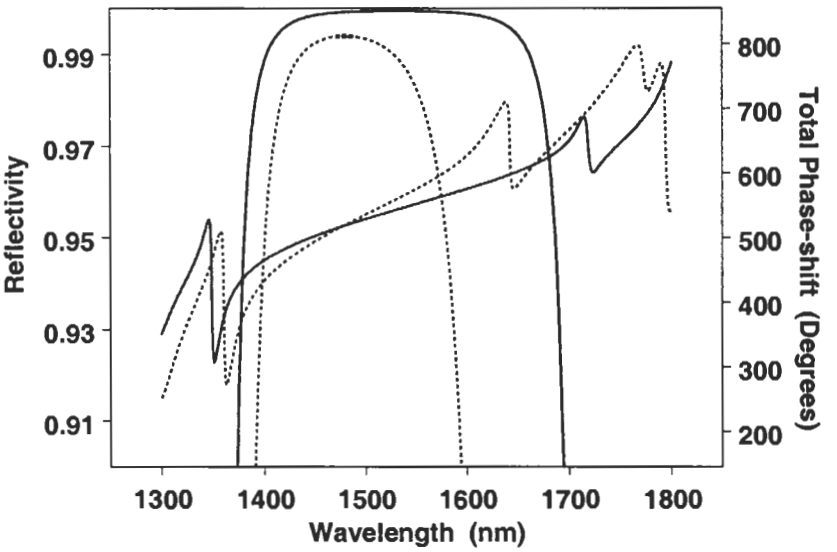

Figure 3. The solid lines are the *s* polarized reflectivity and mirror phase-shift per round trip. The dashed lines are the same quantities for the *p* polarization. The calculated data is for the same $H(LH)^{11}$ dielectric coating on all three mirrors of a three-mirror cavity (see Fig. 2). The different slopes of the two phase-shift curves allow the discrimination of the longitudinal modes of the cavity by measuring the *s*-to-*p* frequency difference.

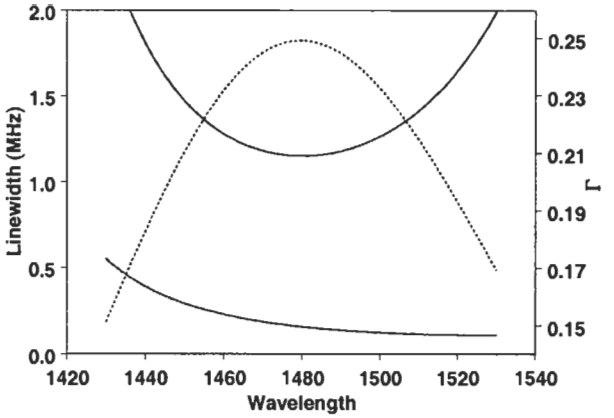

Figure 4. The solid curves are the *p* polarized linewidth (upper) and the *s* polarized linewidth (lower) of the three-mirror cavity. The dashed curve is the figure of merit Γ.

2.4.2 Four-mirror Design

The second cavity that we have considered is a rectangular 4-mirror design as shown in Fig. 5. This configuration has the advantage of four reflections at 45°, slightly enhancing the *s*-to-*p* phase difference. We believe that it may be approximately the same expense to fabricate as a three mirror cavity, even with an additional mirror. This is because it relies on the same standard (90°) angles, and both designs have two mirrors which must be precisely positioned. Furthermore, the same angle of incidence on the mirrors leads to a spectrally wider coating, allowing more widely spaced lasers and subsequently smaller synthetic wavelengths. The calculated linewidth and figure of merit Γ of a 25 cm ring cavity is shown in Fig. 6. The broader spectral width is evident, and the *s* polarization line-width reaches a minimum of 47 kHz at mid-band. The figure of merit reaches a maximum of 0.38 %, but as mentioned above other coating designs may raise Γ to close to 1 % for this cavity configuration.

2.5 Fabrication Tolerances

The angular tolerance of the mirror mating surfaces must be specified in advance for any of these designs, since no adjustment will be possible. In addition the position tolerance of each curved mirror must be specified. The theory of multiple mirror cavity alignment is developed in several references but is fairly involved [22, 23]. Alternatively, we determined the necessary tolerances for the four-mirror cavity design

Figure 5. Four reflections at a 45° angle of incidence enhance the s-to-p dispersion, allowing easier identification of the longitudinal numbers. The beam waists are slightly non-circular due to astigmatism, but in tests a beam from a polarization-preserving fiber was aligned to a square four-mirror cavity such that residual higher-order mode peaks were less than 3 % of the TEM_{00} peak heights.

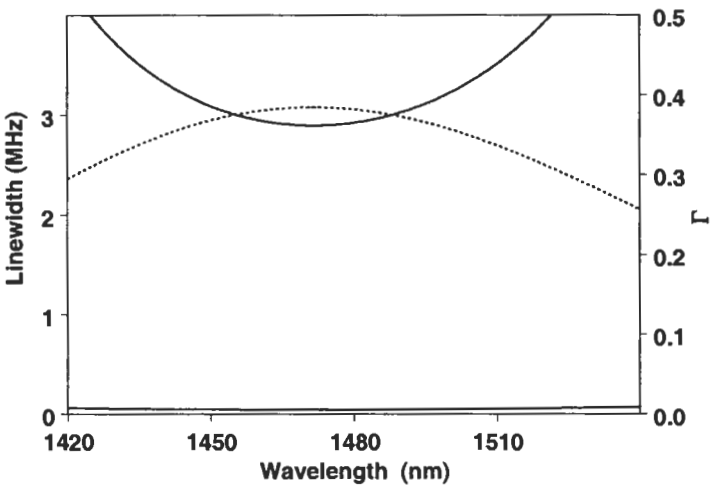

Figure 6. The solid curves are the *p* polarized linewidth (upper) and the *s* polarized line-width (lower) of the rectangular four-mirror 25 cm ring cavity. The dashed curve is the figure of merit, Γ, in percent. The *s* polarized line-width reaches a minimum of 47 kHz at 1470 nm.

by bread-boarding the cavity on an optical table using adjustable mirror mounts. Two flat mirrors and two curved mirrors (50 cm radius) were arranged in a square pattern about 6 cm on a side. Adjacent mirrors were of different types (flat-curved-flat-curved around the square). A mode-matching lens and two turning mirrors were used to couple a collimated beam from an optical fiber to the cavity modes. We were able to align the beam to the cavity TEM_{00} modes, with only a negligible amount of power in the higher-order spatial modes. The cavity mirrors were then misaligned by a known angular amount and the beam re-aligned to the new cavity geometry by use of the input turning mirrors. In this fashion we were able to discern the necessary tolerance on the angular

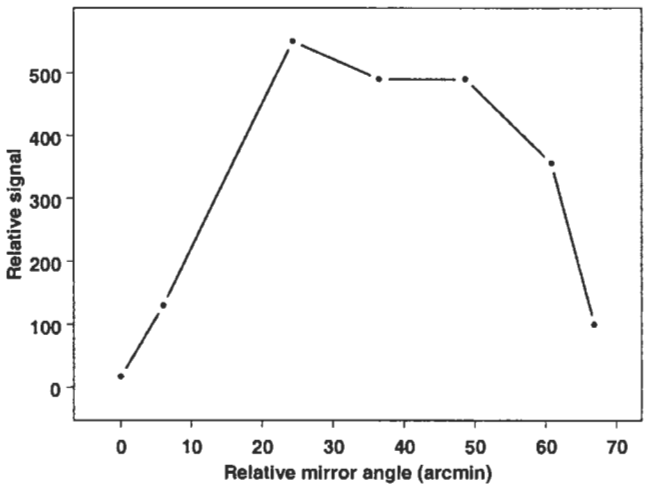

Figure 7. The relative signal level of the TEM_{00} mode as a function of a cavity mirror's angular position. Both dimensions (in the plane of the cavity and orthogonal) resulted in similar data. Both the flat and curved mirrors also resulted in similar data.

alignment of the four cavity mirrors. This is shown in Fig. 7. One of the curved mirrors was held by a micrometer stage, and the position (x-y) tolerance was determined in the same manner. We found that fabrication tolerances of ±5 arc-minutes and ±0.5 mm were sufficient to ensure that the cavity would be in alignment.

3. Prototype Cavity Calibration

A calibration of three different longitudinal modes was performed by measuring the frequency of a laser as it was locked to each mode with the cavity in an evacuated chamber. The residual pressure in the chamber was below 1 mTorr (0.13 Pa), which assured that the refractive index of the medium shifted the resonance frequency by no more than a few parts in 10^{10} from the vacuum value. The cavity temperature was monitored by a thermistor glued to the spacer, with a measurement resolution of 0.1 °C. As the frequency of the prototype-cavity drifted at a rate of $+1.94 \times 10^{-6}$ per °C, temperature uncertainty was the limiting factor in the calibration.

Separate beams for the cavity lock and for the heterodyne measurement were obtained by coupling an extended-cavity laser to an angle-polished fiber, then attaching a 50/50 fiber coupler. One fiber coupler output was directed to a lab some 200 m from the laser, where a mode-locked chromium-doped forsterite laser resides [24]. The second

output was coupled using free-space lenses and mirrors to our prototype cavity inside the vacuum chamber. The chamber had optical-quality windows for the input beam and cavity transmission, and the front-surface reflection and cavity transmission were detected external to the chamber.

The laser was frequency-locked by use of a 100 kHz dither modulation applied via the injection current, and with a feedback-loop bandwidth of approximately 20 kHz. A second, slower, feedback loop was applied to the laser piezoelectric control to keep the average value of the current correction near zero. Although a faster control loop could have been utilized, this implementation was sufficient to keep the laser at the peak of the cavity resonance for hours at a time. The residual uncontrolled frequency noise manifested itself as a small ripple on the cavity transmission of no more than a few percent.

Heterodyne beat-notes between the locked laser and modes of the Cr:forsterite femtosecond laser were observed on a RF spectrum analyzer. The femtosecond laser had a repetition rate and mode spacing of approximately 420 MHz. The mode-locked comb was stabilized by frequency-doubling one mode near 1314 nm and optically phase-locking to a 657 nm frequency-reference laser. The reference laser was provided by the NIST neutral calcium optical frequency reference [25]. The repetition rate was then stabilized by a phase-lock to a low phase-noise laboratory synthesizer which was referenced to the NIST timescale. Once phase-locked, the femtosecond-comb mode frequencies were stable and known, covering the spectrum from approximately 1100 nm to 1800 nm. The actual frequency measurement of the unknown cavity-locked laser frequency consisted of discerning which comb mode was responsible for the heterodyne beat-note, then reading the beat-note frequency with a spectrum analyzer. Details of the apparatus and measurement are reported elsewhere [26].

The frequency and vacuum wavelength values reported in Table 3 were measured at 21.3 °C, although the same resonances were also measured at slightly different temperatures in order to characterize the cavity's drift with temperature. Unfortunately the cavity length actually decreased with temperature at a much higher rate than the ULE spacer expanded, due to the mirror attachment mechanism. As the temperature monitor resolution was 0.1 °C, this implies an inherent temperature uncertainty of ±0.05 °C,

corresponding to a frequency uncertainty of $\pm 97 \times 10^{-9}$, or about ±18 MHz. As this is far larger than the modulation-limited beat-note width of several hundred kilohertz, which is in turn far larger than the uncertainty of the frequency comb, the actual frequency measurement contributed little or nothing to the overall wavelength uncertainty.

The wavelength values reported in Table 3 need to be corrected for use at an ambient pressure and at a temperature other than 21.3 °C. The pressure shift of this particular cavity was not measured experimentally. Furthermore, as the cavity is not reference-quality with optically contacted mirrors, it is reasonable to question the length of time that this calibration will remain accurate. The wavelengths were measured primarily to demonstrate the cavity calibration process.

Table 3. Optical frequency and vacuum wavelengths of three *s* polarized TEM_{00} modes of a prototype wavelength reference at 21.3 °C. The frequency was measured and the wavelength calculated using c = 299,792,458 m/s.

Frequency (THz)	Wavelength (nm)
189.641068 (18)	1580.84143 (15)
189.638238 (18)	1580.86502 (15)
185.130970 (18)	1619.35335 (16)

4. Conclusions

The approach of using stable calibrated resonators to deliver accurate wavelengths in air is technically feasible. We estimate that a total wavelength uncertainty of about $\Delta\lambda/\lambda \leq 3.9 \times 10^{-8}$ could be delivered to interferometer users by such a reference cavity over a ±5 °C temperature range, presently limited by the method of accounting for the mechanical contraction from vacuum to atmospheric pressure. It is possible that this particular uncertainty could be greatly reduced by performing measurements (in air) of a length held fixed by a vacuum interferometer. That concept is not explored in this technical report, but is an area of further research. Other areas for further research include exploring the accuracy versus calibration interval trade-off, and the locking of

visible (red) DFB lasers should they become commercially available. We thank Mark Wippich of New Focus, Inc., and Igor Vayshenker of NIST for the use of a tunable lasers used in part of this work.

References

[1] M. Eickhoff and J. L. Hall, "Real-time precision refractometry: New approaches," Appl. Opt. 36 (6): 1223-1234 (1997).

[2] R. Thibout, S. Topçu, Y. Alayli, and P. Juncar, "A transfer standard of the metre: an air wavelength reference," Eur. Phys. J. – Appl. Phys. 16 (3): 239-245 (2001).

[3] J. A. Stone and A. Stejskal, in *Recent Developments in Traceable Measurements II*, Proc. SPIE 5190, edited by J. Decker and N. Brown, 327-338 (2003).

[4] S. Topçu, Y. Alayli, J. P. Wallerand, and P. Juncar, "Heterodyne refractometer and air wavelength reference at 633 nm," Eur. Phys. J. – Appl. Phys. 24 (1): 85-90 (2003).

[5] R. Dandliker, R. Thalmann, and D. Prongue, "Two-wavelength laser interferometry using super-heterodyne detection," Opt. Lett. 13: 339-343 (1988).

[6] G. P. Barwood, P. Gill, and W. R. C. Rowley, "Laser diodes for length determination using swept-frequency interferometry," Meas. Sci. Tech. 4: 988-994 (1993).

[7] P. E. Ciddor, "Refractive index of air: new equations for the visible and near infrared," Appl. Opt. 35 (9): 1566-1573 (1996).

[8] ULE is a trademark of Corning, Inc. Trade names are mentioned for reference only and do not imply product endorsement by NIST.

[9] Zerodur is a trademark of Schott Glass. Trade names are mentioned for reference only and do not imply product endorsement by NIST.

[10] P. Manson, "High precision free spectral range measurement using a phase modulated laser beam," Rev. Sci. Instrum 70: 3834-3839 (1999).

[11] R. W. Boyd, "Intuitive explanation of the phase anomaly of focused light-beams," J. Opt. Soc. Am., 70 (7): (July 1980).

[12] A. Siegman, *Lasers*, University Science Books (1986).

[13] L. A. Stelmack, C. T. Thurman and G. R. Thompson, "Review of ion-assisted deposition – Research to production," Nucl. Instrum. Methods B37 (8): 787-793 (1989).

[14] S. George, Dept. Chemistry and BioChemistry, University of Colorado, Boulder, private communication.

[15] D. Hils and J. L. Hall, Ultra-stable cavity-stabilized lasers with subhertz linewidth, in Frequency Standards and Metrology, Edited by A. De Marchi, pp. 162-173, Springer-Verlag (1989).

[16] J. C. Bergquist, National Institute of Standards and Technology, Boulder, CO, Private communication.

[17] L. Marmet, A. A. Madej, K. J. Siemsen, J. E. Bernard, and B. G. Whitford, "Precision frequency measurement of the $^2S_{1/2} - {}^2D_{5/2}$ transition of Sr^+ with a 674-nm diode laser locked to an ultrastable cavity," IEEE Trans. Instrum. Meas. 46 (2): 169-173 (1997).

[18] Chr. Tamm, D. Engelke, and V. Buhner, "Spectroscopy of the electric-quadrupole transition $^2S_{1/2}(F=0) - {}_2D_{3/2}(F=2)$ in trapped $^{171}Yb^+$," Phys. Rev. A61 art. 053405 (2000).

[19] F. Riehle, "Use of optical frequency standards for measurements of dimensional stability," Meas. Sci. Technol. 9: 1042-1048 (1998).

[20] M. Andersson, L. Eliasson, and L. R. Pendrill, "Compressible Fabry-Perot refractometer," Appl. Opt. 26 (22): 4835-4840 (1987).

[21] J. Stone and A. Stejskal, "Using helium as a standard of refractive index: correcting errors in a gas refractometer," Metrologia 41: 189-197 (2004).

[22] B. E. Currie, G. E. Stedman, and R. W. Dunn, "Laser stability and beam steering in a nonregular polygonal cavity," Appl. Opt. 41 (9): 1689-1697 (2002).

[23] R. Hauck, H. P. Kortz, and H. Weber, "Misalignment sensitivity of optical resonators," Appl. Opt. 19 (4): 598-601 (1980).

[24] I. Thomann, A. Bartels, K. L. Corwin, N. R. Newbury, L. Hollberg, S. A. Diddams, J. W. Nicholson, and M. F. Yan, "420-MHz Cr:forsterite femtosecond ring laser and continuum generation in the 1-2 μm range," Opt. Lett. 28 (15): 1368 (2003).

[25] C. W. Oates, E. A. Curtis, and L. Hollberg, "Improved short-term stability of optical frequency standards: approaching 1 Hz in 1 s with the Ca standard at 657 nm," Opt. Lett. 25 (21): 1603-1605 (2000).

[26] K. L. Corwin, I. Thomann, T. Dennis, R. W. Fox, W. Swann, E. A. Curtis, C. W. Oates, G. Wilpers, A. Bartels, S. L. Gilbert, L. Hollberg, N. R. Newbury, S. A. Diddams, J. W. Nicholson, and M. F. Yan, "Absolute frequency measurements with a stabilized near-infrared optical frequency comb from a Cr:forsterite laser,", Opt. Lett. 29 (4): 397 (2004).